Molecular Vision 2025; 31:526-537 <http://www.molvis.org/molvis/v31/526>
Received 12 October 2025 | Accepted 18 December 2025 | Published 20 December 2025

Genetic and clinical characterization of suspected retinitis pigmentosa in a cohort of Brazilian patients

Sarah Pereira de Freitas Cenachi,[1] Maria Frasson,[1] Anna Laura Marques Nascentes,[2] Anna Luiza Braga Albuquerque,[3] Rodrigo Rezende Arantes,[2] Virgínia Mares,[1] Luiz Armando Cunha De Marco,[3] Márcio Bittar Nehemy[1]

[1]Department of Ophthalmology, Federal University of Minas Gerais, Belo Horizonte, Brazil; [2]Genetics Service, Federal University of Minas Gerais, Belo Horizonte, Brazil; [3]Department of Surgery, Federal University of Minas Gerais, Belo Horizonte, Brazil

Purpose: To identify causative genetic variants and associated clinical phenotypes in patients of a tertiary referral center in Brazil with suspected retinitis pigmentosa (RP).
Methods: RP diagnosis was established based on predefined clinical criteria. The patients underwent detailed ophthalmologic assessments and multimodal retinal imaging. Genomic DNA was analyzed using a next-generation sequencing (NGS) panel targeting 238 genes associated with inherited retinal diseases.
Results: Among 55 patients, the genetic diagnostic yield was 71% (39/55), with 13 novel variants identified. The most frequently implicated genes were *RHO*, *RPGR*, and *USH2A*, accounting for approximately 50% of genetically diagnosed cases. Fundus autofluorescence revealed patchy hypoautofluorescence surrounding the vascular arcades as the most frequent finding. On spectral-domain optical coherence tomography, the pattern of ellipsoid zone presentation in the central macula was significantly correlated with best-corrected visual acuity ($p<0.001$).
Conclusions: This study delineates the genetic and phenotypic spectrum of RP in a tertiary Brazilian referral center, highlighting the utility of NGS for molecular diagnosis and clinical management.

Retinitis pigmentosa (RP) encompasses a group of progressive inherited retinal diseases (IRDs) characterized by the primary degeneration of rod photoreceptors, followed by the loss of cone photoreceptors [1]. RP is the most prevalent hereditary retinal degenerative disorder, with an estimated global prevalence of 1 in 4,000 individuals and approximately 2.5 million affected worldwide [2,3]. A Brazilian study identified RP as the most common IRD, with the nonsyndromic form accounting for roughly 35% of cases [4]. Nonsyndromic is the main form of RP. In addition, 20% to 30% of patients present with a syndromic form of RP associated with extraocular abnormalities [1].

RP typically manifests during the first or second decade of life, with initial symptoms including nyctalopia, followed by progressive concentric visual field constriction. Central visual function often remains relatively preserved until advanced disease stages. Classic fundus findings include bone spicule pigmentation in the peripheral retina, attenuation of retinal vessels, and optic disc pallor [1].

Retinitis pigmentosa is exceptionally heterogeneous. This includes (1) genetic heterogeneity, with many different genes causing the same disease phenotype; (2) allelic heterogeneity, with many different disease-causing mutations in each gene; (3) phenotypic heterogeneity, with different mutations in the same gene causing different diseases; and (4) clinical heterogeneity, with the same mutation in different individuals producing different clinical consequences, even among members of the same family [5,6]. Nowadays, more than 90 genes have been linked to RP, and this number will likely increase as diagnostic testing techniques improve [7,8]. Furthermore, RP is inherited in a complex manner, involving autosomal dominant inheritance (around 20%), autosomal recessive inheritance (around 30%), and X-linked inheritance (around 10%). Occasionally, digenic inheritance and mitochondrial inheritance also have been reported, highlighting the typical genetic heterogeneity of RP [9].

Despite these complexities, individualized characterization remains essential to inform prognosis, guide genetic counseling, and identify potential therapeutic options. Next-generation sequencing (NGS) has emerged as a powerful diagnostic tool, offering high sensitivity and accuracy in detecting pathogenic variants in IRDs [10-12]. In this study, we applied NGS to a cohort of Brazilian patients with clinically suspected RP, aiming to delineate the genetic landscape and associated clinical features.

Correspondence to: Sarah Pereira de Freitas Cenachi, Department of Ophthalmology 190 Alfredo Balena Avenue, Belo Horizonte - MG - Brazil - 30.190-090; Phone: +55 31 99588-4359; FAX: +55 31 3409-964; email: sarahcenachi@gmail.com

To explore the clinical features, we used data from multimodal imaging assessment, particularly optical coherence tomography (OCT) of the macula. Because the disease involves progressive loss of cones over its course, morphological assessment of photoreceptors in the macular region can be useful for estimating residual central visual function in patients with RP, and OCT is a well established method for in vivo examination of retinal architecture [13]. Several OCT studies in patients with RP have examined the correlation between retinal structure and visual function [14-17].

METHODS

Patient recruitment and clinical evaluation: This study adhered to the principles of the Declaration of Helsinki and was approved by the local ethics committee of the Ezequiel Dias Foundation (Protocol No. 53,981,621.1.3001.9507). Informed consent was obtained from all participants or their legal guardians.

Patients with clinically suspected RP were recruited from the Retina Department at São Geraldo Hospital, Federal University of Minas Gerais, a tertiary referral center in the state of Minas Gerais that provides high-complexity ophthalmologic care to patients from Minas Gerais and other states of Brazil. From June 2022 to May 2024, a total of 55 participants were enrolled, encompassing 36 unrelated patients clinically diagnosed with suspected RP based on the following inclusion criteria: (1) history of nyctalopia and progressive visual acuity loss, (2) visual field constriction, and (3) characteristic fundoscopic findings, including peripheral bone spicule pigmentation, vascular attenuation, and optic disc pallor [1,8]. Demographic data, age of symptom onset, clinical symptoms, family history, and consanguinity status were documented. Syndromic RP cases were excluded [1,9].

The patients underwent comprehensive ophthalmologic evaluation, including best-corrected visual acuity (BCVA), slit-lamp examination, and multimodal retinal imaging. Imaging modalities included color fundus photography (FP; Optos Daytona, Dunfermline, UK, or Topcon, Tokyo, Japan), fundus autofluorescence (FAF; Optos Daytona), and spectral-domain OCT (SD-OCT; Heidelberg Engineering, Heidelberg, Germany). BCVA was assessed using the early treatment diabetic retinopathy study chart and converted to logarithm of the minimum angle of resolution units for statistical analysis. For macular OCT analysis, dense scans as well as vertical and horizontal line scans passing through the fovea were used.

Statistical analyses were conducted on two parameters regarding macular OCT: integrity of the ellipsoid zone and presence of hyperreflective foci in the outer retina. These features were classified according to their location on SD-OCT: within the central 3-mm diameter of the macula, corresponding to the inner ring of the early treatment diabetic retinopathy study grid (central macula), and in the outer retinal layers beyond the central 3 mm (perifoveal macula) [17]. To assess the ellipsoid zone, participants were classified based on the state of the ellipsoid zone (EZ), which could be preserved (when the line was intact), disorganized (when a large part of the integrity of the line was not preserved) [18], or not detected when the zone could not be visualized (not necessarily destroyed but not discernible) [13]. Hyperreflective foci were defined as well circumscribed hyperreflective lesions (with reflectivity at least as bright as the retinal pigment epithelium [RPE] band) and a maximum size of 50 µm. For a more detailed analysis of the correlation between these features and visual acuity, eyes with poor fixation due to extremely low visual acuity (<0.01), vitreomacular traction, macular hole, or macroaneurysm were excluded.

Genetic analysis: Genomic DNA was extracted from saliva samples of all affected individuals. A custom NGS panel targeting 238 genes associated with IRDs was used (Illumina platform). Sequence reads were aligned to the GRCh38 human genome reference, and variants were filtered by proprietary software Abracadabra (Mendelics, Sao Paulo, Brazil) to exclude low-quality calls, common polymorphisms (based on public and internal frequency databases), and variants outside the targeted gene panel, retaining only high-confidence rare variants. DNA from relatives was not available for segregation analysis.

The variants were assessed for pathogenicity according to the American College of Medical Genetics and Genomics guidelines [19]. Annotation used multiple databases, including OMIM, gnomAD, dbSNP, Varsome, and ClinVar.

Variants were classified into five categories: pathogenic, likely pathogenic, variant of uncertain significance, likely benign, and benign. Criteria for classification included minor allele frequency (<0.01% for dominant, <0.5% for recessive variants), previous reports in ClinVar or peer-reviewed literature, in silico deleterious predictions, and consistency with known phenotype and inheritance patterns. Variants not reported in HGMD, ClinVar, or the literature were considered novel [20]. Possible origins of inheritance of each variant were evaluated based on populations in which they had been previously reported, based on gnomAD Exomes.

Statistical analysis: Data were tabulated and analyzed using Microsoft Excel 365 (version 2505, Build 16.0.18827.20102; Microsoft, Redmond, WA). Data were initially analyzed descriptively. For categorical variables, absolute and relative frequencies were presented, while for numerical variables,

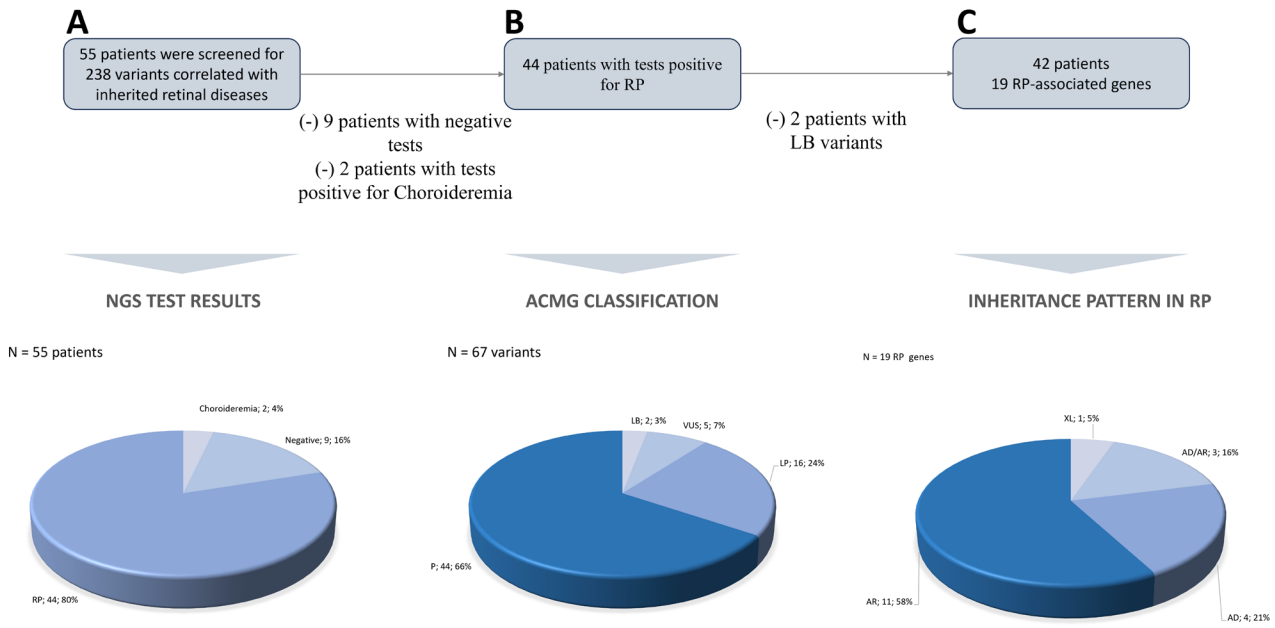

Figure 1. Overview of genetic findings in patients with suspected retinitis pigmentosa. **A**. Flowchart of patient selection and results from NGS. **B**. Variant classification according to ACMG criteria for the 44 genetically evaluated patients. **C**. Distribution of inheritance patterns among identified RP-associated genes. ACMG, American College of Medical Genetics and Genomics; ADRP, autosomal dominant retinitis pigmentosa; ARRP, autosomal recessive retinitis pigmentosa; LB, likely benign; LP, likely pathogenic; NGS, next-generation sequencing; p, pathogenic; RP, retinitis pigmentosa; VUS, variant of uncertain significance; XLRP, X-linked retinitis pigmentosa.

summary measures (mean, quartiles, minimum, maximum, and standard deviation) were reported.

To compare mean visual acuity according to specific characteristics (EZ integrity and presence of hyperreflective foci), a linear mixed-effects model was employed to account for possible dependence between observations from both eyes of the same patient. When significant mean differences were identified, groups with distinct means were determined using ad hoc multiple comparisons under the estimated model, with Bonferroni correction applied to maintain the overall significance level. The linear mixed model assumes data normality, which was assessed using the Kolmogorov–Smirnov test. However, as noted by Gelman and Hill, deviations from normality do not bias the estimates [21]. All statistical tests were performed at a 5% significance level. Analyses were conducted using SPSS version 20.0 (SPSS, Chicago, IL) and STATA version 18 (StataCorp LLC, College Station, TX).

RESULTS

Genetic findings: Of the 55 patients, no pathogenic variants were detected in nine cases, and two cases carried mutations in *CHM*, associated with choroideremia rather than RP. The remaining 44 patients were evaluated for RP-related mutations, yielding 67 variants: 44 pathogenic, 16 likely pathogenic, 5 variants of uncertain significance, and 2 likely benign. After excluding the two cases carrying likely benign variants, 42 patients were retained for analysis. Of these, 39 patients had pathogenic and likely pathogenic variants, resulting in a diagnostic yield of 71% (39/55; Figure 1).

Variants were identified in 19 RP-related genes: *AHI1*, *CLN3*, *CLRN1*, *CRB1*, *EYS*, *FSCN2*, *OPA1*, *PCARE*, *PDE6A*, *PHYC*, *PRCD*, *PRPF31*, *PRPF8*, *PRPH2*, *RHO*, *RPE65*, *RPGR*, *SDCCAG8*, and *USH2A*. The most frequently implicated genes were *RHO*, *RPGR*, and *USH2A*, collectively accounting for nearly 50% of genetically resolved cases. Variants were mapped to known structural domains of the respective proteins (Figure 2).

Autosomal recessive retinitis pigmentosa (ARRP) was the predominant inheritance pattern, present in 11 genes, followed by autosomal dominant RP (ADRP) in 4 genes, mixed ARRP/ADRP in 3 genes, and X-linked RP (XLRP) in 1 gene (Figure 1). Compound heterozygosity was inferred in 14 patients with ARRP, based on clinical presentation suspected of RP, NGS findings of two distinct variants in the same gene, and the known AR inheritance pattern.

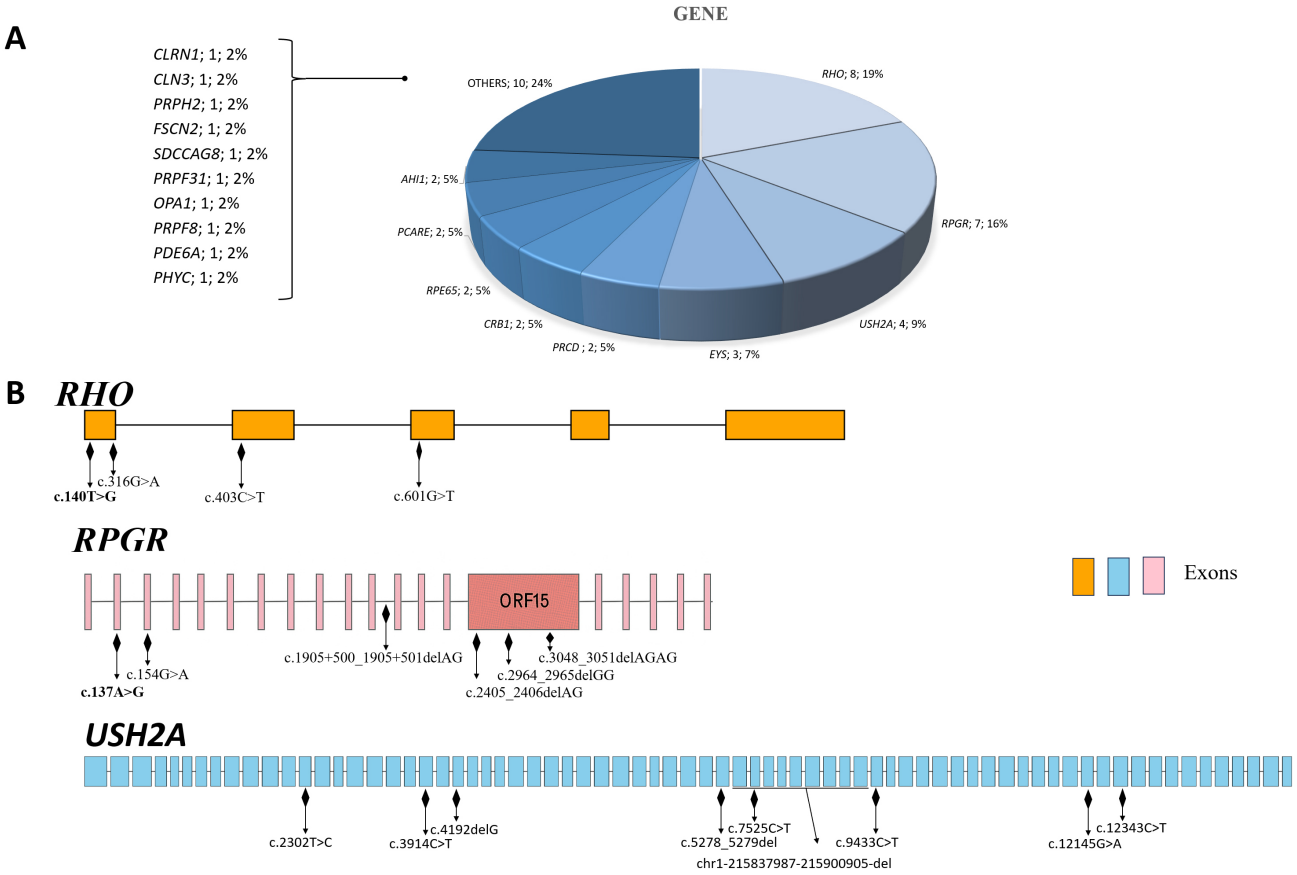

Figure 2. Genetic landscape of the 19 identified RP-associated genes. **A**. Proportional distribution of causative gene variants detected in the study cohort. **B**. Localization of variants within protein structural domains for the three most frequently mutated genes: RHO, RPGR, and USH2A. RP, retinitis pigmentosa.

A total of 65 genetic variants were identified, comprising 44 distinct types. Of these distinct types, 13 were novel mutations (6 missense, 6 frameshift, and 1 insertion), 27 variants were previously reported (14 missense, 7 frameshift, 5 nonsense, 1 intronic), and 4 copy number variants CNVs could not be conclusively categorized as novel. Novel variants were identified in 13 genes: *AHI1*, *CRB1*, *EYS*, *FSCN2*, *PCARE*, *PDE6A*, *PHYC*, *PRCD*, *RHO*, *RPE65*, *RPGR*, *SDCCAG8*, and *USH2A*. Comprehensive genetic findings are summarized in Appendix 1.

Causative mutation in a gene involved in other inherited retinal diseases: Two sisters were found to carry the c.940+1G>T mutation in *CHM*, consistent with X-linked choroideremia. Both had been clinically misdiagnosed with RP based on overlapping features, including nyctalopia, peripheral pigmentation, vascular narrowing, and optic disc pallor. Based on genetic results, their diagnoses were revised to choroideremia.

Demographics: Among the 42 analyzed patients, 21 were male and 21 were female, with ages ranging from 9 to 90 years (mean: 39±18 years). Age of symptom onset ranged from 5 to 52 years (mean: 25±14 years; Appendix 2). Consanguinity was reported in 7% of patients (P2, P25, and P34), and a family history of visual impairment was present in 52% (22/42; Appendix 1).

Clinical findings: All 42 patients reported visual symptoms. Nyctalopia was the most frequent complaint, reported by 86% of patients (36/42), followed by photophobia in 19% (8/42). BCVA ranged from 20/25 to light perception, with a median of 20/50. Myopia was the predominant refractive error, observed in 59% of eyes (47/80) among the 40 patients who underwent refraction. Bilateral cataracts were identified in 33% of patients (14/42), and among them, 36% (n=5 patients) had undergone lensectomy in at least one eye (Appendix 2).

Fundus photography: FP was performed in 39 patients, yielding 78 eyes for analysis. Optic disc pallor was observed

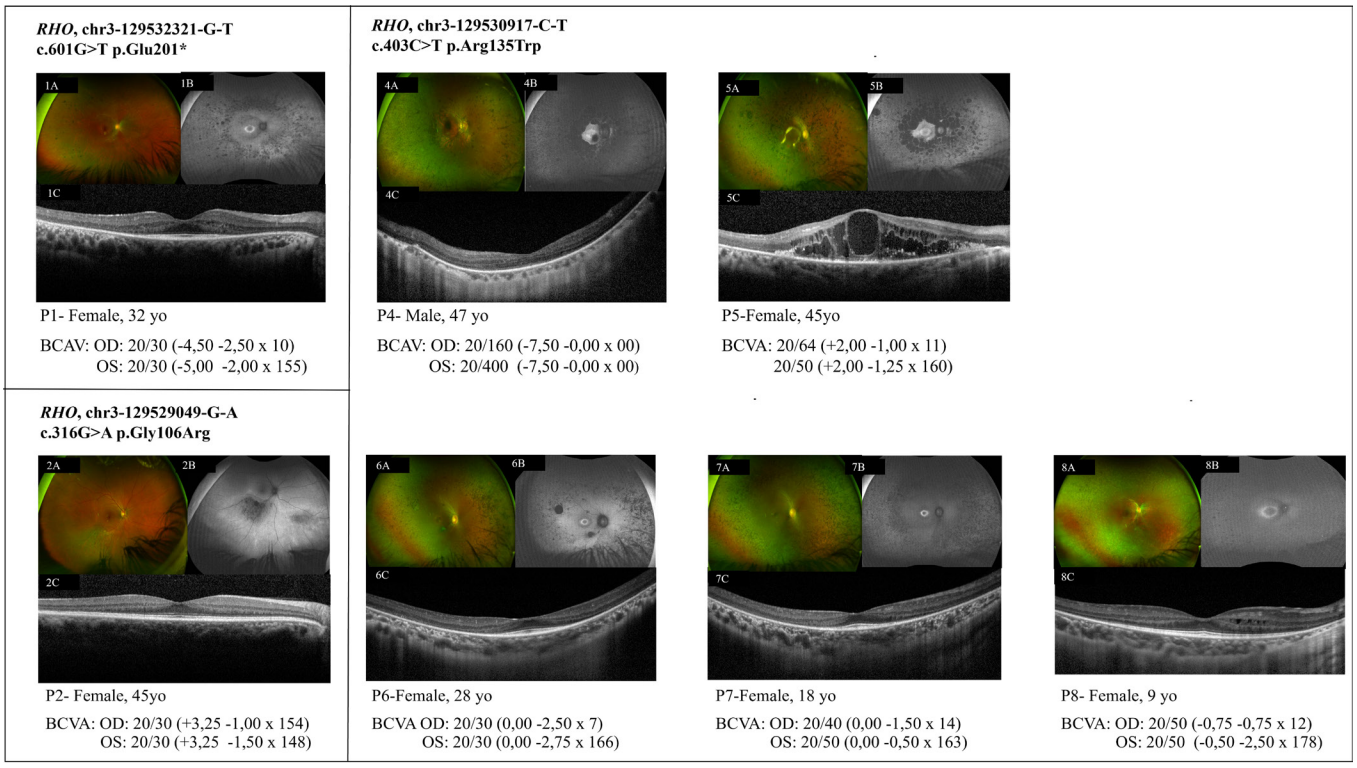

Figure 3. Genetic and clinical characterization of patients with the RHO gene variant in the cohort. The patients harbor three different variants: c.601G>T in P1, c.316G>A in P2, and c.403C>T in P4 to P8, the latter being related patients (P4 is the sibling of P5, who is the mother of P6, P7, and P8). Images include color fundus photography (A), fundus autofluorescence (FAF; B), and optical coherence tomography (OCT; C) of the right eye. Color fundus photographs show peripheral pigmentation, vascular attenuation, and optic disc pallor in both eyes of all patients. FAF imaging highlights the presence of the parafoveal hyperautofluorescent ring (e.g., P1B, P6B, P7B, P8B), corresponding on OCT to the demarcation between areas of central photoreceptor preservation and regions where the outer retina is structurally disrupted (e.g., P1C, P6C, P7C, P8C). Additional OCT findings include large cysts in the internal and external layers, and surrounding hyperreflective plaques in the outer retina in P5C correspond to a macroaneurysm. In 8C, cysts are identified in both the inner and outer retinal layers. This figure illustrates phenotypic heterogeneity: patient P2, who carries the c.316G>A variant, exhibited sectoral retinal involvement, whereas other patients with different variants in the same gene showed diffuse retinal involvement. Clinical heterogeneity is also evident, as patient P8, aged 9 years, carries the same mutation as her older sisters but presents with more pronounced macular edema.

in 92% of eyes (72/78) and vascular attenuation in 90% (70/78). Retinal pigment epithelium alterations were present in all eyes, with peripheral pigmentation in the form of bone spicules observed in 97% (76/78). Two eyes showed no fundus pigmentation but exhibited RPE rarefaction in the peripheral retina. All findings were bilateral, highlighting the symmetric presentation characteristic of inherited retinal diseases (Appendix 2, Figure 3, and Figure 4).

Fundus autofluorescence: FAF was performed in 38 patients. Due to poor fixation, the examination could not be completed in 4 eyes, resulting in 72 eyes analyzed. In the macular region, 35% of eyes (25/72) exhibited a hyperautofluorescent ring, consistent with Robson-Holder ring [22], and 14% (10/72) showed patchy hypoautofluorescence surrounding the fovea, indicative of bull's-eye atrophy [23]. In the peripheral retina, 79% of eyes (57/72) demonstrated patchy hypoautofluorescence surrounding the vascular arcades. Representative FAF findings are shown in Figure 3 and Figure 4.

Spectral-domain optical coherence tomography: SD-OCT was performed in 39 of the 42 patients, totaling 78 eyes analyzed. Retinal cysts were identified in 49% of eyes (38/78), with small cysts accounting for 84% (32/38). An epiretinal membrane was present in 47% of eyes (37/78), with bilateral involvement in 17 of the 20 affected patients. Macular holes were observed in three eyes from three different patients: one eye had a full-thickness macular hole with associated sensory shallow macular detachment (P29), while two had lamellar holes with epiretinal proliferation and adjacent epiretinal membrane (P11 and P42).

Central macular thickness was measured by SD-OCT in 74 of the 78 eyes analyzed, with 4 eyes excluded due to poor fixation. Central macular thickness values ranged from 96 to 630 µm, with a mean of 251 µm and a median of 247 µm. SD-OCT findings are shown in Appendix 1 and Figure 3.

Regarding the correlation between visual acuity and EZ integrity features and the presence of hyperreflective foci in the macular region, 65 eyes from 34 patients were included in the statistical analysis. The data indicate that alterations in the EZ in the central macula on OCT are associated with visual acuity ($p<0.001$). The mean BCVA in the group with a nondetected EZ was significantly lower than that of the preserved EZ and disorganized EZ groups, with no significant difference observed between the latter two. The analysis

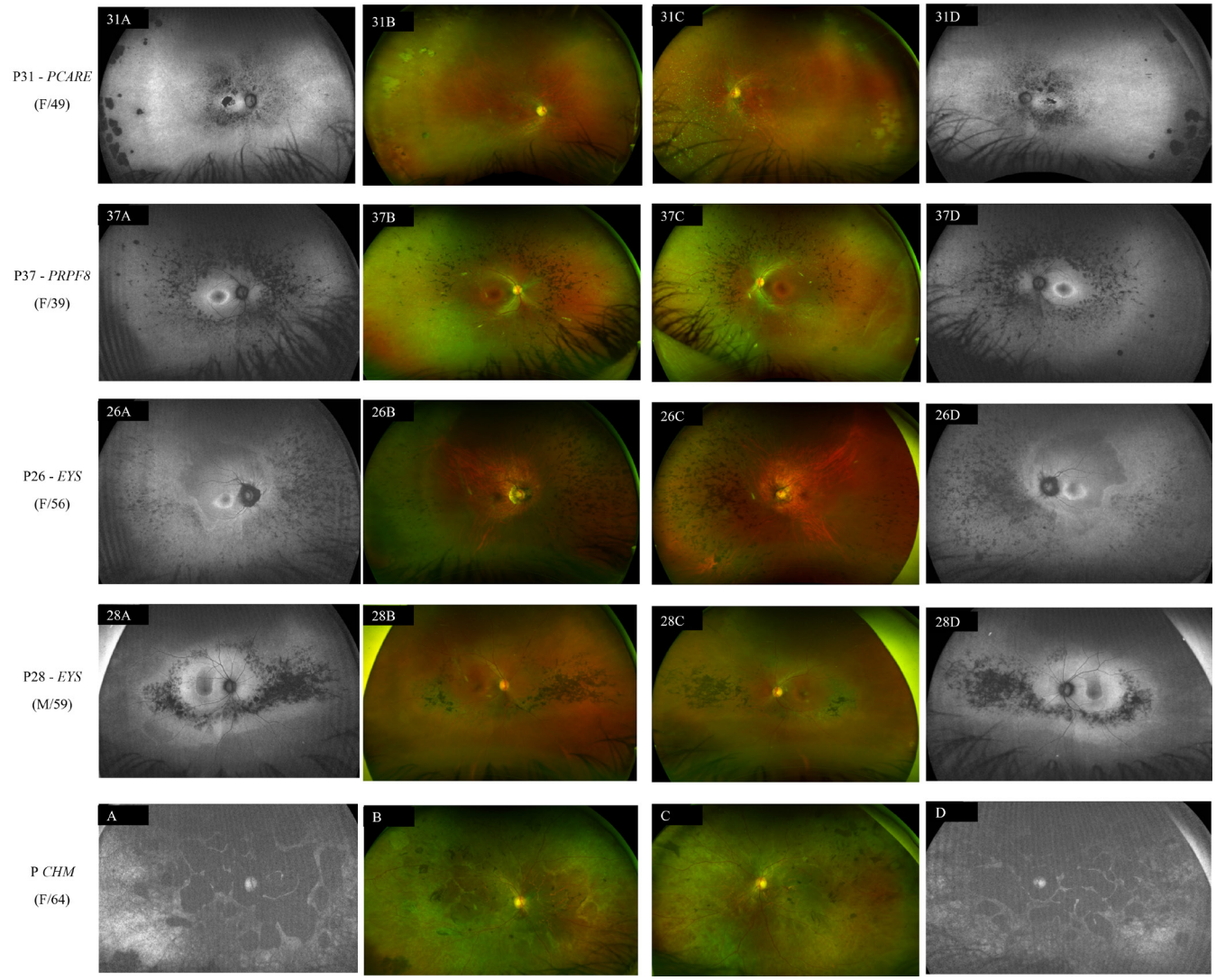

Figure 4. Multimodal imaging of patients carrying RP-associated gene variants: PCARE (P31), PRPF8 (P37), EYS (P26, P28), and CHM. Images include fundus autofluorescence (FAF; A and D) and fundus photography (B and C). Panels A and B correspond to the right eye; panels C and D correspond to the left eye. In patients P31 (PCARE) and P37 (PRPF8), FAF images (P31A, P31D; P37A, P37D) show hypoautofluorescent patches surrounding the arcades, corresponding to areas of retinal pigmentation and atrophy that may be less evident on color fundus photography (P31B, P31C; P37B, P37D). In patients P26 and P28, both harboring EYS variants, distinct FAF patterns previously associated with this gene were observed: a "broad-banded hyperautofluorescent leading edge" in P26 and an "infinity sign" in P28. Fundus photographs of these patients demonstrate peripheral pigmentation, vascular attenuation, and optic disc pallor in both patients. In the patient with a pathogenic CHM variant (choroideremia), FAF imaging revealed scalloped mid-peripheral chorioretinal atrophy—a hallmark feature of the disease. Fundus photography displayed overlapping features with RP, including peripheral pigmentation, vessel narrowing, and optic disc pallor. RP, retinitis pigmentosa.

Table 1. Association between SD-OCT features and visual acuity in a nonsyndromic retinitis pigmentosa cohort.

SD-OCT features	Number of eyes analyzed (sample %)	Mean visual acuity (LogMAR)	p
Ellipisoid zone in central macula			<0,001
Preserved EZ	28/65 (43,1%)	0,24±0,14ł	
Disorganized EZ	26/65 (40,0%)	0,49±0,35ł	
Not detected EZ	11/65 (16,9%)	0,84±0,42§	
Elipisoid zone in perifoveal macula			0.212
Preserved EZ	2/65 (3,1%)	0,36±0,25	
Disorganized EZ	13/65 (20,0%)	0,25±0,13	
Not detected EZ	50/65 (76,9%)	0,49±0,39	
Hyperreflective foci (HRF) in central macula			0.236
Absence of HRF	49/65 (75,4%)	0,40±0,37	
Presence of HRF	16/65 (24,6%)	0,58±0,30	
Hyperreflective foci in perifoveal macula			0.095
Absence of HRF	30/65 (46,2%)	0,32±0,29	
Presence of HRF	35/65 (53,8%)	0,55±0,39	

p - descriptive level of the mixed-effects regression model (*p* - mixed linear model); statistically significant finding is represented in bold. § and ł indicate significantly different means based on ad hoc multiple comparisons with Bonferroni correction. The features were classified according to their location on SD-OCT: within the central 3 mm diameter of the macula, corresponding to the inner ring of the ETDRS grid (central macula), and in the outer retinal layers beyond the central 3 mm (perifoveal macula).

of other variables in relation to BCVA did not reach statistical significance (Table 1 and Figure 5).

DISCUSSION

RP is the most prevalent form of IRD, with over 90 genes currently implicated in its pathogenesis [24]. The genetic heterogeneity of RP is profound, encompassing multiple inheritance modes, variable penetrance, and phenotypic diversity—even among individuals carrying the same pathogenic variant [5]. As clinical features often overlap with other IRDs, accurate molecular diagnosis remains critical for definitive classification, prognosis, genetic counseling, and potential therapeutic stratification [9]. In the present cohort, a targeted NGS panel yielded a genetic diagnosis in 71% of patients, corroborating its role as a powerful diagnostic tool, as reported in previous studies [9,25,26]. Moreover, we identified 13 novel variants, expanding the known mutational spectrum associated with RP.

Variants in three genes—RHO, RPGR, and USH2A—accounted for nearly half of the cases resolved by genetics. These genes have also been reported among the most prevalent in epidemiological studies on RP conducted both within and outside Brazil [4,9,27-30] (Table 2). In our cohort, 35% of the patients were related, and this information was used to explore the clinical heterogeneity of RP (Figure 3 and Appendix 1).

RHO, encoding rhodopsin, was the most frequently implicated gene. Rhodopsin is a G protein-coupled receptor localized to rod photoreceptor outer segment discs, where it mediates phototransduction upon activation by light [7]. Mutations in *RHO* are the predominant cause of ADRP, accounting for approximately 25% to 30% of ADRP cases [31]. In the present study, *RHO* variants were identified in eight patients: c.601G>T in patient 1 (P1), c.316G>A in P2, c.140T>G in P3, and c.403C>T in P4 to P8, who were related. The onset of visual impairment ranged from 5 to 37 years of age. Among the patients carrying RHO variants, P2 exhibited sectoral peripheral retinal involvement, whereas the others demonstrated global peripheral retinal involvement, showing phenotypic heterogeneity. Moreover, clinical heterogeneity was observed; notably, P8, aged 9 years, carries the same mutation as her older sisters but presents a more severe disease spectrum, with more pronounced macular edema and worse visual acuity (Figure 3). Preservation of the fovea was observed in most of these cases, consistent with the "OCT-based transition zone" model proposed by Hood et al., in which the outer nuclear layer remains partially intact over the central photoreceptors but disappears beyond the foveal region [32]. FAF imaging frequently revealed the presence of the Robson-Holder ring. This hyperautofluorescent circular band surrounding the fovea represents the transition zone

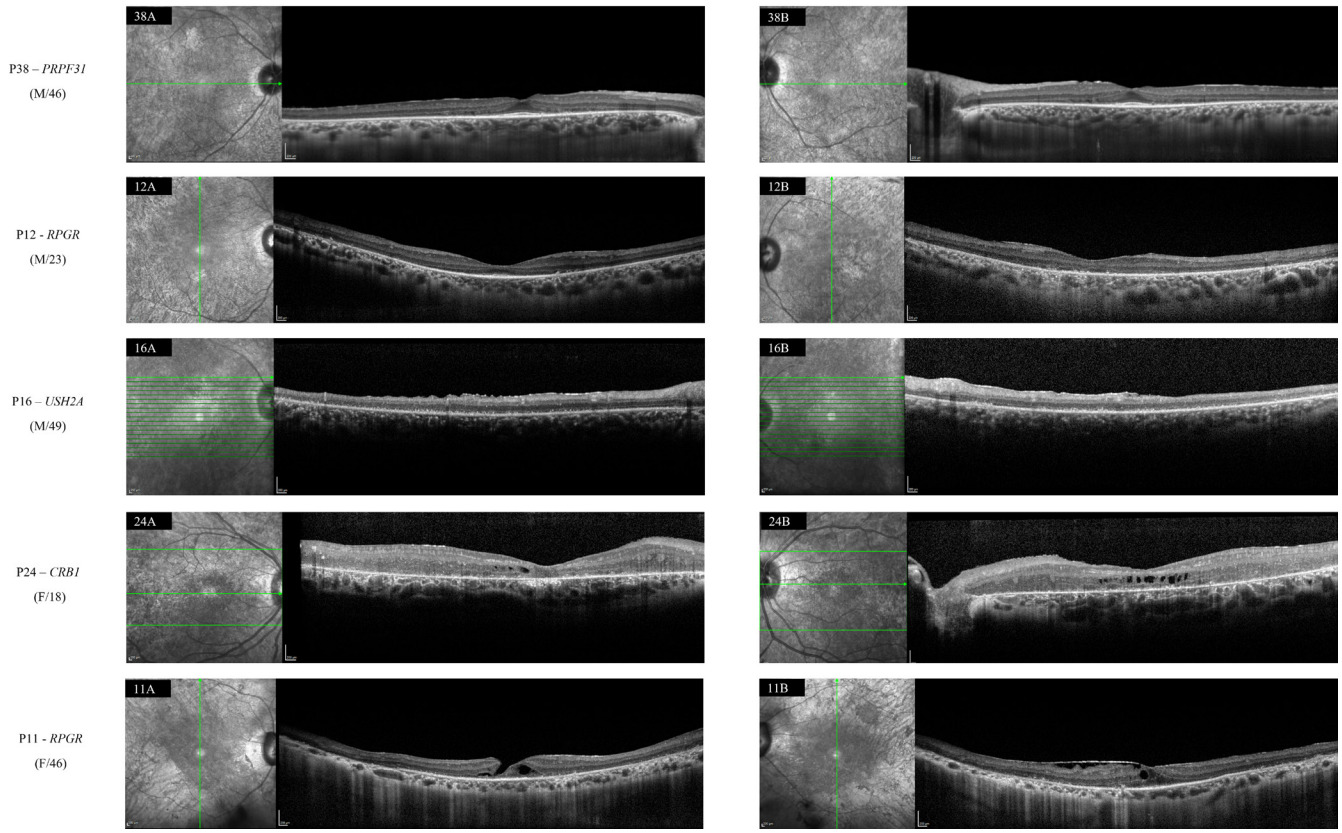

Figure 5. SD-OCT imaging of patients carrying RP-associated gene variants: PRPF31 (P38), RPGR (P12), USH2A (P16), CRB1 (P24), RPGR (P11). Panel A corresponds to the right eye (OD); panel B corresponds to the left eye (OS). Presentation of the ellipsoid zone (EZ): In P38, the central macula showed a preserved EZ, whereas the perifoveal macula exhibited a not detected EZ in both eyes (OU); in P12, the central macula displayed a disorganized EZ in OD and a not detected EZ in OS; the perifoveal macula showed a not detected EZ in OU. Presentation of hyperreflective foci (HRF): In P16, HRF were observed in the perifoveal macula in OU; in P24, HRF were observed in the central macula and in the perifoveal macula in OU. In P11, a lamellar macular hole was present in the OD and an epiretinal membrane in the OS. RP, retinitis pigmentosa.

between relatively preserved central photoreceptors and degenerating peripheral retina [22].

The second most frequently mutated gene was *RPGR*, associated with approximately 70% of XLRP cases [33]. RPGR is localized to the connecting cilia of photoreceptors and plays a key role in ciliary trafficking, although its precise function remains incompletely understood. XLRP due to *RPGR* mutations typically manifests early and progresses rapidly, often with profound visual impairment [34]. In our study, *RPGR* variants were identified in seven patients—five males and two females. Age of onset ranged from 5 to 29 years. OCT findings in affected individuals frequently showed macular atrophy of photoreceptor layers. Female carriers demonstrated variable phenotypes, consistent with previous reports of XLRP carrier expressivity [35]. One female patient harboring the c.2405_2406delAG variant exhibited significant retinal involvement, including bilateral loss in the EZ, retinal cysts, an epiretinal membrane, and a unilateral macular hole (Figure 5).

The third most common gene was *USH2A*, previously reported as a major contributor to both syndromic and nonsyndromic RP in various populations [36]. Located on chromosome 1q41, *USH2A* encodes usherin, a basement membrane protein involved in cochlear and retinal development [37]. Four patients carried *USH2A* variants—three with compound heterozygous mutations and one with a homozygous variant. Symptom onset was later than in *RHO* or *RPGR* carriers (range: 38–49 years). No patient reported hearing loss at the time of evaluation; however, audiological assessment was recommended.

The variants were most commonly reported in European and African populations. Yet, several were also reported in Asian, admixed American, and Ashkenazi Jewish populations, reflecting Brazil's population genetic diversity. Brazil's

Table 2. Selected previous studies in non- syndromic retinitis pigmentosa cohorts.

Study Author(s) by year	Country	Molecularly tested (N)	Molecularly solved cohort (N)	Different disease-causing genes	Most frequently implicated genes
Current study, 2025	Brazil	55 individuals/36 families	71% (39/55) individuals	19	RHO (19%), *RPGR* (16%), *USH2A* (9%), *EYS* (7%)
Costa et al., 2017	Brazil	16 individuals	56% (9/16) individuals	8	RPGR (22%), *RHO* (11%), *CRB1* (11%), PRPF31 (11%)
Motta et al., 2018	Brazil	191 individuals	63% (121/191) individuals	31	RPGR (16%), *EYS* (13%), *USH2A* (9%), *CERKL (6%), RP1 (76%)*
Chukwunalu et al., 2025	Portugal	352 individuals/268 families	57% (202/352) individuals	40	EYS (28.7%), *RPGR* (7.9%), *USH2A* (6.4%), *RPE65* (5.9%), *RHO* (5.5%)
Bouzidi et al., 2022	North Africa	NI	76 families:	23	
			45 non-Jewish families	20	MERTK (18%), *PDE6B* (11%), CERKL (9%), RP1 (9%)
			31 Jewish families	7	FAM161A (58%), *EYS (*23%), *RDH12* (6%)
Jin et al., 2023	China	75 individuals/75 families	44% (33/75) individuals	14	USH2A (22%), *CYP4V2* (19%), *RPGR* (16%), *EYS* (6%)
Birtel et al., 2018	Germany	116 individuals/116 families	70% (81/116) individuals	30	RPGR (10%), *EYS* (9%), *PRPF31* (7%), *USH2A* (6%)

Legend: NI: Not Informed

genetic architecture represents the world's largest recently admixed population, rooted in an intricate interplay between native indigenous populations, colonization effects, assertive mating, and modern immigration [38]. This cohort represents the mosaic of global haplotypes represented in Brazilian genomic diversity.

Widefield imaging technology was employed in this study to document retinal changes, enhancing the characterization of RP subtypes. FAF analysis identified hypoautofluorescent patches surrounding the arcades, corresponding to areas of pigmentation and retinal atrophy that may not be as evident on retinography (Figure 4). Identification of this finding may be useful for early detection of suspected RP cases and for differential diagnosis, such as uveitis. FAF can also facilitate RP subtype characterization in conjunction with genetic testing. In some patients, FAF patterns such as the "infinity sign" (peripapillary and macular sparing) and "broad-banded hyperautofluorescent leading edge" were observed—patterns previously associated with *EYS* mutations (Figure 4) [39].

SD-OCT provides high-resolution cross-sectional imaging of retinal morphology and is a valuable tool for assessing disease severity and progression in RP [40-42]. This disease is characterized by progressive degeneration of the photoreceptor and RPE layers, initially manifesting in the mid-peripheral retina and subsequently extending toward the macula [1,18].

In the present study, we observed a significant correlation between the degree of EZ disruption in the central 3 mm of the macula and worsening visual acuity, reinforcing the importance of central photoreceptor integrity as a structural marker of visual function [13]. In contrast, the presence of hyperreflective foci in this region did not show statistical significance in our study, although previous reports have identified them as potential biomarkers of RP progression [16,17]. This discrepancy may be related to our sample size, which may still be insufficient for this level of analysis.

Future studies incorporating functional assessments such as visual field testing and microperimetry, along with the application of artificial intelligence—similar to advances achieved in geographic atrophy associated with age-related macular degeneration—may yield important insights into retinal dystrophies [43].

Notably, two patients harboring a pathogenic *CHM* splice-site variant (c.940+1G>T) were initially misdiagnosed

with RP. The *CHM* gene causes X-linked choroideremia, a chorioretinal dystrophy that clinically mimics RP but is pathophysiologically distinct. FAF imaging in these patients revealed scalloped mid-peripheral chorioretinal atrophy, a hallmark of choroideremia (Figure 4) [9,44]. This underscores the importance of multimodal retinal imaging and molecular testing in achieving an accurate diagnosis.

Additionally, mutations were identified in genes associated with syndromic disorders. These included *AHI1*, associated with Joubert syndrome [45], and *CLN3*, linked to Batten disease [46]. Although the patients reported no systemic symptoms beyond ocular manifestations, given the potential for an association with broader systemic diseases, further genetic investigation was recommended.

This study has certain limitations. The NGS panel employed does not detect variants in deep intronic or regulatory regions, nor does it provide robust CNV characterization. Co-segregation analysis was not feasible, limiting the ability to confirm variant phase in recessive cases. Finally, as discussed in the OCT analysis, the relatively small sample size restricts broader genotype–phenotype correlation analyses, although it remains representative of a rare disease.

Conclusions: This study provides a comprehensive molecular and clinical characterization of patients with suspected RP from a tertiary referral center in Brazil. The 71% diagnostic yield highlights the effectiveness of NGS panels in IRD evaluation. Thirteen novel variants were identified, contributing to the expanding mutational landscape of RP. The findings emphasize the importance of integrating genetic testing with clinical and imaging data to refine diagnoses, guide patient management, and enable personalized therapeutic approaches.

APPENDIX 1. POTENTIAL CAUSATIVE VARIANTS AND CLINICAL CHARACTERISTICS OF 42 PATIENTS WITH SUSPECTED RETINITIS PIGMENTOSA.

To access the data, click or select the words "Appendix 1."

APPENDIX 2. SUPPLEMENTARY DATA OF POTENTIAL CAUSATIVE VARIANT AND CLINICAL CHARACTERISTICS OF THE 42 PATIENTS.

To access the data, click or select the words "Appendix 2." Table containing the complementary set of clinical information of the 42 patients subject to the present study.

ACKNOWLEDGMENTS

Disclosure statement: The authors report no conflicts of interest. The authors alone are responsible for the content and writing of this article. Funding: The genetic tests were partially funded by Novartis AG.

REFERENCES

1. Verbakel SK, van Huet RAC, Boon CJF, den Hollander AI, Collin RWJ, Klaver CCW, Hoyng CB, Roepman R, Klevering BJ. Non-syndromic retinitis pigmentosa. Prog Retin Eye Res 2018; 66:157-86. [PMID: 29597005].

2. Koyanagi Y, Akiyama M, Nishiguchi KM, Momozawa Y, Kamatani Y, Takata S, Inai C, Iwasaki Y, Kumano M, Murakami Y, Omodaka K, Abe T, Komori S, Gao D, Hirakata T, Kurata K, Hosono K, Ueno S, Hotta Y, Murakami A, Terasaki H, Wada Y, Nakazawa T, Ishibashi T, Ikeda Y, Kubo M, Sonoda KH. Genetic characteristics of retinitis pigmentosa in 1204 Japanese patients. J Med Genet 2019; 56:662-70. [PMID: 31213501].

3. Hartong DT, Berson EL, Dryja TP. Retinitis pigmentosa. Lancet 2006; 368:1795-809. [PMID: 17113430].

4. Motta FL, Martin RP, Filippelli-Silva R, Salles MV, Sallum JMF. Relative frequency of inherited retinal dystrophies in Brazil. Sci Rep 2018; 8:15939-[PMID: 30374144].

5. Daiger SP, Sullivan LS, Bowne SJ. Genes and mutations causing retinitis pigmentosa. Clin Genet 2013; 84:132-41. [PMID: 23701314].

6. de Freitas Cenachi SP, Frasson M, Mares V, Arantes RR, Albuquerque ALB, Marques Nascentes AL, De Marco LAC, Nehemy MB. Genetics and phenotypes of *RPE65* mutations in inherited retinal degeneration: A study from a tertiary eye care center in Brazil. Mol Vis 2025; 31:45-54. [PMID: 40384766].

7. Vingolo EM, Mascolo S, Miccichè F, Manco G. Retinitis Pigmentosa: From Pathomolecular Mechanisms to Therapeutic Strategies. Medicina (Kaunas) 2024; 60:189-[PMID: 38276069].

8. Nguyen XT, Moekotte L, Plomp AS, Bergen AA, van Genderen MM, Boon CJF. Retinitis Pigmentosa: Current Clinical Management and Emerging Therapies. Int J Mol Sci 2023; 24:7481-[PMID: 37108642].

9. Jin B, Li J, Yang Q, Tang X, Wang C, Zhao Y, Zheng F, Zhang Y, Ma J, Yan M. Genetic characteristics of suspected retinitis pigmentosa in a cohort of Chinese patients. Gene 2023; 853:147087[PMID: 36464167].

10. Gao FJ, Li JK, Chen H, Hu FY, Zhang SH, Qi YH, Xu P, Wang DD, Wang LS, Chang Q, Zhang YJ, Liu W, Li W, Wang M, Chen F, Xu GZ, Wu JH. Genetic and Clinical Findings in a Large Cohort of Chinese Patients with Suspected Retinitis Pigmentosa. Ophthalmology 2019; 126:1549-56. [PMID: 31054281].

11. Adams DR, Eng CM. Next-Generation Sequencing to Diagnose Suspected Genetic Disorders. N Engl J Med 2018; 379:1353-62. [PMID: 30281996].
12. Consugar MB, Navarro-Gomez D, Place EM, Bujakowska KM, Sousa ME, Fonseca-Kelly ZD, Taub DG, Janessian M, Wang DY, Au ED, Sims KB, Sweetser DA, Fulton AB, Liu Q, Wiggs JL, Gai X, Pierce EA. Panel-based genetic diagnostic testing for inherited eye diseases is highly accurate and reproducible, and more sensitive for variant detection, than exome sequencing. Genet Med 2015; 17:253-61. [PMID: 25412400].
13. Aizawa S, Mitamura Y, Baba T, Hagiwara A, Ogata K, Yamamoto S. Correlation between visual function and photoreceptor inner/outer segment junction in patients with retinitis pigmentosa. Eye (Lond) 2009; 23:304-8. [PMID: 18188175].
14. Witkin AJ, Ko TH, Fujimoto JG, Chan A, Drexler W, Schuman JS, Reichel E, Duker JS. Ultra-high resolution optical coherence tomography assessment of photoreceptors in retinitis pigmentosa and related diseases. Am J Ophthalmol 2006; 142:945-52. [PMID: 17157580].
15. Matsuo T, Morimoto N. Visual acuity and perimacular retinal layers detected by optical coherence tomography in patients with retinitis pigmentosa. Br J Ophthalmol 2007; 91:888-90. [PMID: 17314147].
16. Huang CH, Yang CH, Lai YJ, Hsiao CK, Hou YC, Yang CM, Chen TC. Hyperreflective foci as important prognostic indicators of progression of retinitis pigmentosa. Retina 2022; 42:388-95. [PMID: 34510128].
17. Félix R, Gouveia N, Bernardes J, Silva R, Murta J, Marques JP. Prognostic impact of hyperreflective foci in nonsyndromic retinitis pigmentosa. Graefes Arch Clin Exp Ophthalmol 2024; 262:2851-8. [PMID: 38578334].
18. Martins EADS, Rodrigues GD, Ivama KJ, Pereira MC, Texeira CHM, Amaral RAS, Sallum JMF. Multimodal imaging in retinitis pigmentosa related to the EYS gene. Arq Bras Oftalmol 2024; 88:S0004–27492025000300306[PMID: 39607159].
19. Richards S, Aziz N, Bale S, Bick D, Das S, Gastier-Foster J, Grody WW, Hegde M, Lyon E, Spector E, Voelkerding K, Rehm HL. ACMG Laboratory Quality Assurance Committee. Standards and guidelines for the interpretation of sequence variants: a joint consensus recommendation of the American College of Medical Genetics and Genomics and the Association for Molecular Pathology. Genet Med 2015; 17:405-24. [PMID: 25741868].
20. Aguirre J, Padilla N, Özkan S, Riera C, Feliubadaló L, de la Cruz X. Choosing Variant Interpretation Tools for Clinical Applications: Context Matters. Int J Mol Sci 2023; 24:11872-[PMID: 37511631].
21. Gelman A, Hill J. Data Analysis Using Regression and Multilevel/Hierarchical Models. New York: Cambridge University Press; 2007. 625 p.
22. Robson AG, Tufail A, Fitzke F, Bird AC, Moore AT, Holder GE, Webster AR. Serial imaging and structure-function correlates of high-density rings of fundus autofluorescence in retinitis pigmentosa. Retina 2011; 31:1670-9. [PMID: 21394059].
23. Zahid SB. Kari. Schlegel, Dana. Pennesi, Mark E. Michaelides, Michel. Heckenlively, John. Jayasundera, Thiran. Retinal Dystrophy Gene Atlas Springer; 2018. 279 p.
24. Kim YJ, Kim YN, Yoon YH, Seo EJ, Seo GH, Keum C, Lee BH, Lee JY. Diverse Genetic Landscape of Suspected Retinitis Pigmentosa in a Large Korean Cohort. Genes (Basel) 2021; 12:675-[PMID: 33946315].
25. Neveling K, Collin RW, Gilissen C, van Huet RA, Visser L, Kwint MP, Gijsen SJ, Zonneveld MN, Wieskamp N, de Ligt J, Siemiatkowska AM, Hoefsloot LH, Buckley MF, Kellner U, Branham KE, den Hollander AI, Hoischen A, Hoyng C, Klevering BJ, van den Born LI, Veltman JA, Cremers FP, Scheffer H. Next-generation genetic testing for retinitis pigmentosa. Hum Mutat 2012; 33:963-72. [PMID: 22334370].
26. Xu Y, Guan L, Shen T, Zhang J, Xiao X, Jiang H, Li S, Yang J, Jia X, Yin Y, Guo X, Wang J, Zhang Q. Mutations of 60 known causative genes in 157 families with retinitis pigmentosa based on exome sequencing. Hum Genet 2014; 133:1255-71. [PMID: 24938718].
27. Birtel J, Gliem M, Mangold E, Müller PL, Holz FG, Neuhaus C, Lenzner S, Zahnleiter D, Betz C, Eisenberger T, Bolz HJ, Charbel Issa P. Next-generation sequencing identifies unexpected genotype-phenotype correlations in patients with retinitis pigmentosa. PLoS One 2018; 13:e0207958[PMID: 30543658].
28. Chukwunalu O, Ambrósio AF, Carvalho AL, Quinn PMJ, Marques JP, Alves CH. Genetic Landscape of Nonsyndromic Retinitis Pigmentosa in Portugal. Adv Exp Med Biol 2025; 1468:81-6. [PMID: 39930177].
29. Costa KA, Salles MV, Whitebirch C, Chiang J, Sallum JMF. Gene panel sequencing in Brazilian patients with retinitis pigmentosa. Int J Retina Vitreous 2017; 3:33-[PMID: 28912962].
30. Bouzidi A, Charoute H, Charif M, Amalou G, Kandil M, Barakat A, Lenaers G. Clinical and genetic spectrums of 413 North African families with inherited retinal dystrophies and optic neuropathies. Orphanet J Rare Dis 2022; 17:197-[PMID: 35551639].
31. Yan Z, Yao Y, Li L, Cai L, Zhang H, Zhang S, Xiao Q, Wang X, Zuo E, Xu C, Wu J, Yang H. Treatment of autosomal dominant retinitis pigmentosa caused by RHO-P23H mutation with high-fidelity Cas13X in mice. Mol Ther Nucleic Acids 2023; 33:750-61. [PMID: 37621413].
32. Hood DC, Lazow MA, Locke KG, Greenstein VC, Birch DG. The transition zone between healthy and diseased retina in patients with retinitis pigmentosa. Invest Ophthalmol Vis Sci 2011; 52:101-8. [PMID: 20720228].
33. Becherucci V, Bacci GM, Marziali E, Sodi A, Bambi F, Caputo R. The New Era of Therapeutic Strategies for the Treatment of Retinitis Pigmentosa: A Narrative Review of Pathomolecular Mechanisms for the Development of Cell-Based Therapies. Biomedicines 2023; 11:2656-[PMID: 37893030].

34. Cehajic-Kapetanovic J, Xue K, Martinez-Fernandez de la Camara C, Nanda A, Davies A, Wood LJ, Salvetti AP, Fischer MD, Aylward JW, Barnard AR, Jolly JK, Luo E, Lujan BJ, Ong T, Girach A, Black GCM, Gregori NZ, Davis JL, Rosa PR, Lotery AJ, Lam BL, Stanga PE, MacLaren RE. Initial results from a first-in-human gene therapy trial on X-linked retinitis pigmentosa caused by mutations in RPGR. Nat Med 2020; 26:354-9. [PMID: 32094925].

35. Salvetti AP, Nanda A, MacLaren RE. RPGR-Related X–Linked Retinitis Pigmentosa Carriers with a Severe "Male Pattern". Ophthalmologica 2021; 244:60-7. [PMID: 32434206].

36. Zhu T, Chen DF, Wang L, Wu S, Wei X, Li H, Jin ZB, Sui R. *USH2A* variants in Chinese patients with Usher syndrome type II and non-syndromic retinitis pigmentosa. Br J Ophthalmol 2021; 105:694-703. [PMID: 32675063].

37. Santana EE, Fuster-García C, Aller E, Jaijo T, García-Bohórquez B, García-García G, Millán JM, Lantigua A. Genetic Screening of the Usher Syndrome in Cuba. Front Genet 2019; 10:501-[PMID: 31231422].

38. Nunes K, Araújo Castro E Silva M, Rodrigues MR, Lemes RB, Pezo-Valderrama P, Kimura L, de Sena LS, Krieger JE, Catoia Varela M, de Azevedo LO, Aranha Camargo LM, Ferreira RGM, Krieger H, Bortolini MC, Mill JG, Sacuena P, Guerreiro JF, de Souza CMB, Veronese FV, Vianna FSL, Comas D, Pereira AC, Pereira LV, Hünemeier T. Admixture's impact on Brazilian population evolution and health. Science 2025; 388:eadl3564[PMID: 40373151].

39. Kominami T, Tan TE, Ushida H, Jain K, Goto K, Bylstra YM, Sajiki AF, Mathur RS, Ota J, Lim WK, Nishiguchi KM, Fenner BJ. Fundus autofluorescence features specific for EYS-associated retinitis pigmentosa. PLoS One 2025; 20:e0318857[PMID: 39970144].

40. Menghini M, Cehajic-Kapetanovic J, MacLaren RE. Monitoring progression of retinitis pigmentosa: current recommendations and recent advances. Expert Opin Orphan Drugs 2020; 8:67-78. [PMID: 32231889].

41. Battaglia Parodi M, La Spina C, Triolo G, Riccieri F, Pierro L, Gagliardi M, Bandello F. Correlation of SD-OCT findings and visual function in patients with retinitis pigmentosa. Graefes Arch Clin Exp Ophthalmol 2016; 254:1275-9. [PMID: 26472300].

42. Gong Y, Xia H, Zhang A, Chen LJ, Chen H. Optical coherence tomography biomarkers of photoreceptor degeneration in retinitis pigmentosa. Int Ophthalmol 2021; 41:3949-59. [PMID: 34304340].

43. Enzendorfer ML, Schmidt-Erfurth U. Artificial intelligence for geographic atrophy: pearls and pitfalls. Curr Opin Ophthalmol 2024; 35:455-62. [PMID: 39259599].

44. Li S, Guan L, Fang S, Jiang H, Xiao X, Yang J, Wang P, Yin Y, Guo X, Wang J, Zhang J, Zhang Q. Exome sequencing reveals CHM mutations in six families with atypical choroideremia initially diagnosed as retinitis pigmentosa. Int J Mol Med 2014; 34:573-7. [PMID: 24913019].

45. Nguyen TT, Hull S, Roepman R, van den Born LI, Oud MM, de Vrieze E, Hetterschijt L, Letteboer SJF, van Beersum SEC, Blokland EA, Yntema HG, Cremers FPM, van der Zwaag PA, Arno G, van Wijk E, Webster AR, Haer-Wigman L. Missense mutations in the WD40 domain of *AHI1* cause non-syndromic retinitis pigmentosa. J Med Genet 2017; 54:624-32. [PMID: 28442542].

46. Zhang X, Xu K, Shi J, Xie Y, Li N, Yan W, Jin ZB, Li Y. Phenotypic variability observed in a Chinese patient cohort with biallelic variants in the *CLN* genes. Mol Vis 2024; 30:175-87. [PMID: 39563673].